

**ASTROMETRY FROM SPACE: AN OVERVIEW  
OF THE EUROPEAN SPACE AGENCY'S  
*HIPPARCOS* SATELLITE**

By

Kirby D. Runyon

A thesis submitted in partial fulfillment of the requirements for  
the degree of

Bachelor of Arts

Houghton College

June 2008

Signature of Author.....

Department of Physics  
June 14, 2008

.....  
Dr. Mark Yuly  
Professor of Physics  
Thesis Supervisor

.....  
Dr. Brandon Hoffman  
Assistant Professor of Physics

**ASTROMETRY FROM SPACE: AN OVERVIEW OF THE  
EUROPEAN SPACE AGENCY'S *HIPPARCOS*  
SATTELITE**

By

Kirby D. Runyon

Submitted to the Department of Physics  
on June 14, 2008 in partial fulfillment of the  
requirement for the degree of  
Bachelor of Arts

**Abstract**

The European Space Agency's Hipparcos satellite was launched in 1989 to provide a high-precision catalogue of stellar astrometric data, including parallaxes and luminosities, from above Earth's dimming and distorting atmosphere. Despite the satellite failing to reach its intended geosynchronous orbit, its mission successfully measured astrometric characteristics of 120,000 stars and photometric and less accurate astrometric properties of approximately one million stars. Since the mission's end, the data have been reduced into several catalogues that have proven useful in determining other astrometric and astrophysical properties of stellar phenomena. This report will describe the motivation for and details of the Hipparcos mission, the data reduction, the applications of these data, and the prospects for future space-based astrometry missions.

Thesis Supervisor: Dr. Mark Yuly  
Title: Professor of Physics

## TABLE OF CONTENTS

<i>Chapter 1 Introduction</i> .....	5
<i>Chapter 2 Motivation</i> .....	7
<i>Chapter 3 The Hipparcos Satellite</i> .....	10
<b>3.1 History</b> .....	10
<b>3.2 Mission Plan</b> .....	11
<b>3.3 Hipparcos Payload</b> .....	11
<b>3.4 Tycho Experiment</b> .....	14
<b>3.5 Support Systems</b> .....	16
3.5.1 Attitude and Maneuvering .....	16
3.5.2 Telecommunication .....	17
3.5.3 Thermal Control [13] .....	18
3.5.4 Power Generation and Management .....	18
3.5.5 Gyroscopes .....	19
<b>3.6 The Hipparcos Launch and Mission Performance</b> .....	19
<i>Chapter 4 Data Reductions - NDAC, FAST, and Tycho</i> .....	20
<b>4.1 NDAC</b> .....	20
<b>4.2 FAST</b> .....	21
<b>4.3 The Hipparcos Catalog</b> .....	23
<b>4.4 Tycho</b> .....	23
<i>Chapter 5 Data Applications from the Hipparcos Satellite</i> .....	24
<b>5.1 Interferometric Angular Diameters of Mira Variables with the Hubble Space Telescope</b> .....	24
<b>5.2 Galactic Kinematics of Cepheids from Hipparcos Proper Motions</b> .....	24
<b>5.3 Ages of Globular Clusters from Hipparcos Parallaxes of Local Subdwarfs</b> .....	25
<b>5.4 The Mass and Radius of 40 Eridani B From Hipparcos: An Accurate Test of Stellar Interior Theory</b> .....	25
<b>5.5 The Hipparcos Distances of Open Clusters and their Implication on the Local Variations of the Ratio</b> .....	26
<b>5.6 Seismic Analysis of the Planet-Hosting StarArae</b> .....	26
<b>5.7 Ice Age Epochs and the Sun's Path Through the Galaxy</b> .....	26
<i>Chapter 6 Future Prospects and Conclusion</i> .....	28
<b>6.1 Future Prospects</b> .....	28
<b>6.2 Conclusion</b> .....	28

## TABLE OF FIGURES

Figure 1.	Schematic of parallax.....	8
Figure 2.	Geometric schematic showing trigonometric relationships.....	9
Figure 3.	Optics schematic for primary Hipparcos experiment.....	12
Figure 4.	Hipparcos' fields of view and rotation.....	13
Figure 5.	Plot showing phase difference of stars.....	14
Figure 6.	Tycho/star mapper schematic.....	15
Figure 7.	Photograph and sketch of the Hipparcos Satellite.....	16

## Chapter 1

### INTRODUCTION

Astrometry the branch of astronomy concerned with measuring the positions of stars relative to each other and Earth. Its uses range from helping determine astrophysical properties of stellar objects such as galactic kinematics [1] and stellar seismic activity [2] to acquiring accurate positions and motions of land masses on Earth [3]. The distances to nearby stars are measured using parallax angles caused by Earth's motion around the Sun. The first recorded attempt [4] at measuring parallax and thereby directly confirming the Copernican system was by Bradley in 1728, though he did not succeed. It was not until the mid-1800s that Bessel [3] recorded the parallax angle of 61 *Cygni* with a Koenigsberg heliometer. These early attempts were hampered by the intrinsic difficulty for human vision to discern such small angles.

In the late 1970s, over a century after Bessel's success, the European Space Agency (ESA—pronounced “EE-suh”) conducted a feasibility study of a space-based astrometry mission which would be freed of the distorting and dimming effects of Earth's atmosphere. The convection currents and fluidity of Earth's atmosphere alter the path of starlight to the ground in addition to absorbing much of the light; peering through the atmosphere is akin to looking at the bottom of a disturbed pond. Such a spacecraft would need precision pointing, high resolution telescopes and imagers, and a stable thermal environment to reduce flexure of the optics and electronic noise. It should be noted in the nearly three decades since, advancements in technology such as adaptive optics and segmented telescope mirrors have partially addressed the problems for which a space-based mission was needed.

In 1980 ESA decided implement a space-based astrometry satellite; construction began in 1984, with a launch in 1989. The name of the spacecraft was *Hipparcos*, named after the ancient Greek astronomer Hipparchus who lived in the second century BC. It is also an acronym for High Precision Parallax Collecting Satellite. Hipparchus' work [3] established the precession of Earth's axis, as well as more accurately predicted the motion of the Moon and the apparent motion of the Sun. The Hipparcos mission succeeded in producing a catalogue of astrometric measurements more

accurate than was initially anticipated, despite the spacecraft not achieving the intended orbit. The data was and continues to be used in areas ranging from stellar interior theory [5] to helping determine the properties of ice age epochs on Earth [6].

## *Chapter 2*

### MOTIVATION

The purpose of astrometry is twofold: to provide a non-rotating stellar reference frame with which astronomical objects may be compared, and to provide an observational basis for studying other astrophysical properties of stellar phenomena. The applications [7] of astrometry include the ability to derive stellar masses, understand intra- and extra-galactic kinematics, determine stellar age, and derive stellar birth locations. The purpose of the Hipparcos satellite and the resulting data catalogues was to further astrometric measurement to precisions hitherto unattained. From 1850 to the Hipparcos mission, astrometric precision improved from 0.01 arcsec to 0.002 arcsec [3].

The Hipparcos mission sought to eliminate the problems that historically compromised astrometric data. These include distortion by Earth's atmosphere; instrument flexure caused by gravity causing optics to flex non-uniformly as telescope position is changed; uncontrolled thermal environments which exacerbated instrument flexure; and limited visibility from only viewing the part of the celestial sphere afforded by a particular telescope's hemisphere. The spacecraft circumvented [8] these challenges by being in space above the distorting effects of the atmosphere; operating in a microgravity environment in which optics and instruments are unaffected by gravitational flexure; by maintaining a well-controlled thermal environment; and by being in view of the entire celestial sphere over the course of its mission. Operating a mission in space introduces a new set of problems [3], however. These included maneuvering system vibrations; launch vehicle, orbit, and telecommunications considerations; cosmic ray bombardment; and the lack of observational flexibility afforded by the observing scheme.

Parallax is the means in astrometry to acquire relatively nearby stellar distances. Other distance measuring techniques, such as the period-luminosity relationship of Cepheid variables, are calibrated from the parallax-measured distances. In other words, parallax forms the foundation on which all other distances measuring techniques are based. Knowing distances to stars allows for stellar properties to be deduced based on the distance and luminosity of a star. For example, if two stars appear to have the same magnitude but parallax shows one star as farther away, the more distant star

must have a higher absolute magnitude. This implies the star is more massive than the other and will therefore have a shorter lifetime.

Parallax measurement works as follows. As Earth changes position in its solar orbit, the apparent locations of relatively nearby stars appears to shift slightly when compared with much further astronomical objects. These apparent shifts are usually measured in milliarcseconds (mas), or  $1/3,600,000$  of a degree. Distances, in parsecs (pc), may be derived from these angular shifts. A parsec is the distance of an object that appears to shift one arcsecond tangentially to the line of sight compared to the distant background after the observing platform (usually Earth) has moved one astronomical unit. As seen in Figure 1, the basic practice is to measure the angular shift of the star in question over the course of a year and divide the maximum angle by two, since opposite sides of Earth's orbit are two AU's apart. It does not matter how the star is positioned relative to the plane of Earth's orbit (the Ecliptic).

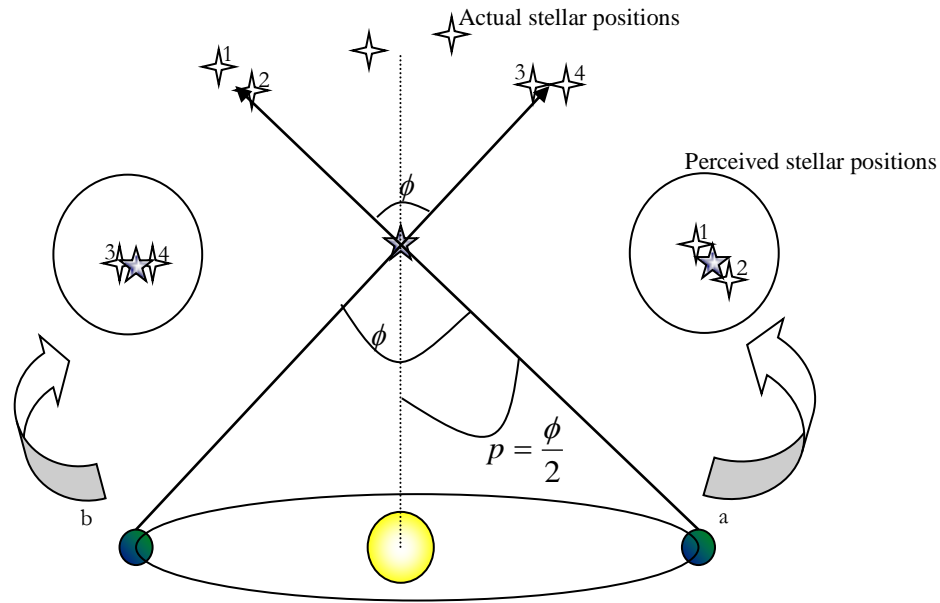


Figure 1. Schematic of parallax. (a) Astrometric measurements are taken of a star's position relative to much further stars; the view is shown in the circle. (b) One-half of an Earth orbit later the position is found again, and it appears to have shifted position relative to the much further stars.



This parallax angle  $p$ , in arcseconds, can be inverted to give the approximate distance  $d$  in parsecs, using the small angle approximation. The derivation is therefore, noting Figure 2,

	$\frac{r}{d} = \sin p$	
Expand sine in a trigonometric series.	$\frac{r}{d} = p - \frac{p^3}{3} + \frac{p^5}{5} - \frac{p^7}{7} + \dots$	
Neglect higher order terms since $p$ is small and $p'' \ll p$ (small angle approximation).	$\frac{r}{d} = p$	
Recall $r = 1$ (Fig. 2) and solve for $d$ . We therefore arrive at Eq. 1.	$d = \frac{1}{p}$	Eq. 1.

In other words, a parsec is the necessary distance for one AU to subtend one arcsec. One parsec is approximately 3.26 light years, with a light year being the distance light travels in one year, or approximately 9.46 billion km.

Parallax is only effective for stars relatively close to the Sun, since for very distant stars the size of Earth's orbit becomes insignificant making the parallax angle much too small to measure with current technology. Hipparcos' designed parallax accuracy was 0.002 arcsec for the main experiment. The limiting magnitude was designed to be 12.4.

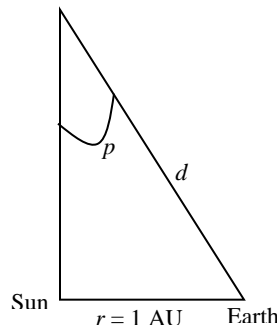


Figure 2. Geometric schematic showing trigonometric relationships. The angle between the measurements in (a) and (b) is halved and used in Eq. 1 to calculate the distance.

THE HIPPARCOS SATELLITE

**3.1 History**

Planning [3, 8] for a space astrometry mission began in the late 1960s when astronomers realized ground-based astrometry—with then-current technology—had reached its pinnacle due to Earth’s dimming and turbulent atmosphere. This realization prompted a feasibility study for a space astrometry mission by the European Space Agency (ESA) in the late 1970s. ESA determined that technology had advanced to the point where a large number of faint stars could be studied and that the astrophysical results of a space astrometry mission would be of great interest to astronomers. Additionally, ESA decided the Ariane launch vehicle ought to be used; the Ariane allowed for a heavier payload than was originally assumed and the ability to reach geostationary orbit. Geostationary orbit would be advantageous since the Earth would only block a small portion of the celestial sphere from that altitude of approximately 35,786 kilometers and since it meant only one ground station was needed. The launch vehicle decision was adopted by the science team in their spacecraft planning. Hipparcos became an official mission in 1980 in which participation was mandatory by all ESA member countries. Hardware development [9] began in early 1984 by ESA’s contractor for Hipparcos, Matra Marconi Space of Toulouse, France, and was completed in May of 1988.

The spacecraft launched from ESA’s French Guiana launch site aboard an Ariane 4 rocket on August 8, 1989. The successful launch placed Hipparcos in an elliptical transfer orbit [7], from which the apogee boost motor was to circularize the spacecraft’s orbit into a geosynchronous orbit. Ignition of this stage failed, however, and the spacecraft remained in its highly eccentric 507 x 35,888 km orbit [10] with a period of about 10 hours [11]. This restricted observations to times when the spacecraft was away from perigee (when Earth blocked a large portion of the celestial sphere) and when the spacecraft traveled through the van Allen radiation belts since this increased instrument noise. Because of this, data collection time was restricted by 50 to 60%, although this was later improved to 35 to 40% through re-writing much of the spacecraft’s software. The spacecraft’s mission ended in March 1993, having lasted 7 months longer than planned. Mission

termination occurred due to on-board computer failure and problems with the guidance system's gyroscopes.

### 3.2 Mission Plan

The original plan [12] for Hipparcos was to enter a geosynchronous orbit and precisely determine the parallax, position, proper motion, and photometric properties of 120,000 predetermined stars—called program stars—to magnitude 12.5 and an accuracy of 2 mas (per year, in the case of proper motion) over a mission duration of 2.5 years. Despite the failure to reach the proper orbit, stellar parameters were obtained to an accuracy of 1 mas. A complimentary experiment onboard the spacecraft, called the Tycho experiment [13], sought to obtain two-color photometric data for about 1,000,000 stars down to 12th magnitude in blue and full-visible spectrum light. The plan for the Tycho experiment was revised after the failure of the apogee boost motor. The spacecraft's passage through the van Allen radiation belts which surround Earth decreased the signal-to-noise ratio of the star-mapper, which was a photomultiplier tube, and resulted in a 50% loss in the original Tycho experiment data. With the “revised” Tycho mission the original goals were more than met. This data was coupled with astrometric data with accuracy of 0.03 arcsec and magnitude accuracy of 0.03 mag.

### 3.3 Hipparcos Payload

The core of the science payload [3, 8, 14]—both for the Hipparcos payload and the Tycho experiment—was the 29 cm diameter Schmidt telescope with a focal length of 1.4 m and a split beam-combining flat aspheric mirror. A Schmidt telescope uses a spherical primary mirror which is easier to manufacture than a higher-quality parabolic mirror. To correct for the resulting spherical aberration in images, a corrector lens is placed at the opening of the telescope. Images are recorded at the prime focus—that is, the focal plane of the mirror. Schmidt telescopes have low aberration and a large field of view.

As shown in Figure 3, light from fields of view (FOV) separated by 58 degrees was conveyed by baffles to a beam-combing flat aspheric mirror, then to a flat folding mirror, and then projected on the spherical primary mirror. The image detector (a photomultiplier tube) sat at the prime focus behind a hole in the correcting mirror. In this way two  $0.9^\circ \times 0.9^\circ$  FOVs were viewed simultaneously. The spacecraft rotated about its  $\hat{x}$ -axis once every 128 minutes and so allowed the two FOVs to sweep out great circles on the celestial sphere. (A great circle is a circle drawn on a

sphere dividing it evenly into hemispheres.) A rough position of each of the 120,000 program stars was known before the mission; Hipparcos' onboard computer "knew" which stars to expect at a particular moment in time to cross the field of view, though this information was transmitted from the ground periodically.

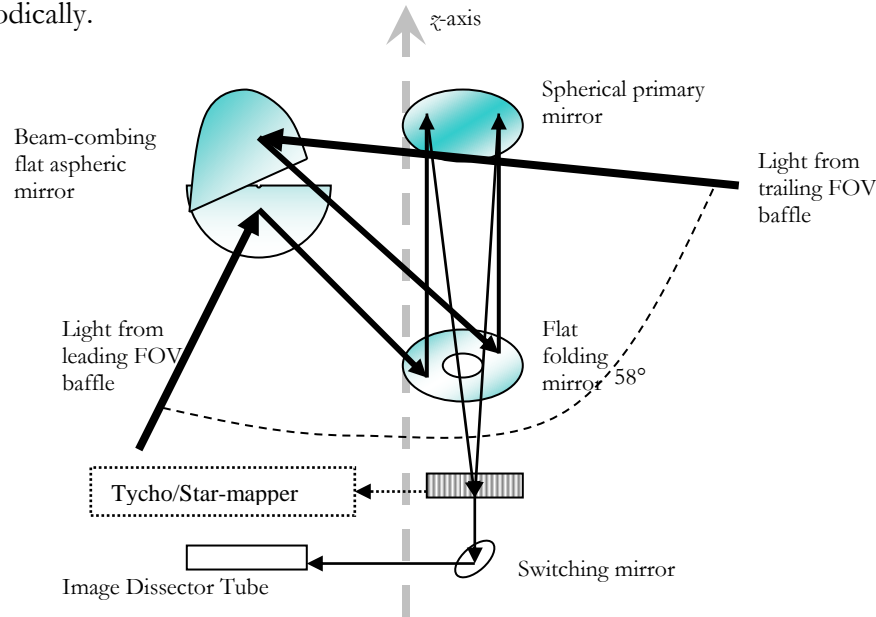


Figure 3. Optics schematic [8] for the primary Hipparcos experiment. Light comes in from the two field of views (darkest arrows) and is incident on different portions of the beam-combining mirror. Then it reflects (medium-dark arrows) toward the flat folding mirror before reflecting (medium arrows) off the primary mirror. Finally it reflects (light arrows) through a hole in the flat folding mirror to the image detector.

At any one time four or five program stars were visible through the combined view of each FOV with each star taking 19.2 seconds to transit across. The angular separation of stars could be calculated based on the 58 degree separation of the FOVs and their apparent separation on the focal plane, as shown in Figure 4. For example, if two stars, one in each FOV, had their light combined on the focal plane and one image was precisely on top of the other their separation would be exactly that of the FOVs—58 degrees. About 20 minutes after a star was viewed in the leading FOV it would appear in the trailing FOV and thereby compared with yet more stars. The spin and  $z$ -axis of Hipparcos were coincident and this joint axis precessed so that over several years the entire sky would be imaged. Even as the satellite orbited Earth this axis was fixed at approximately 43 degrees to the direction of the Sun and had a precession period of about eight weeks. By determining the angular separation of a star with many other stars, creating a vast network of interrelated angular separations, a very accurate catalogue of star coordinates could be calculated.

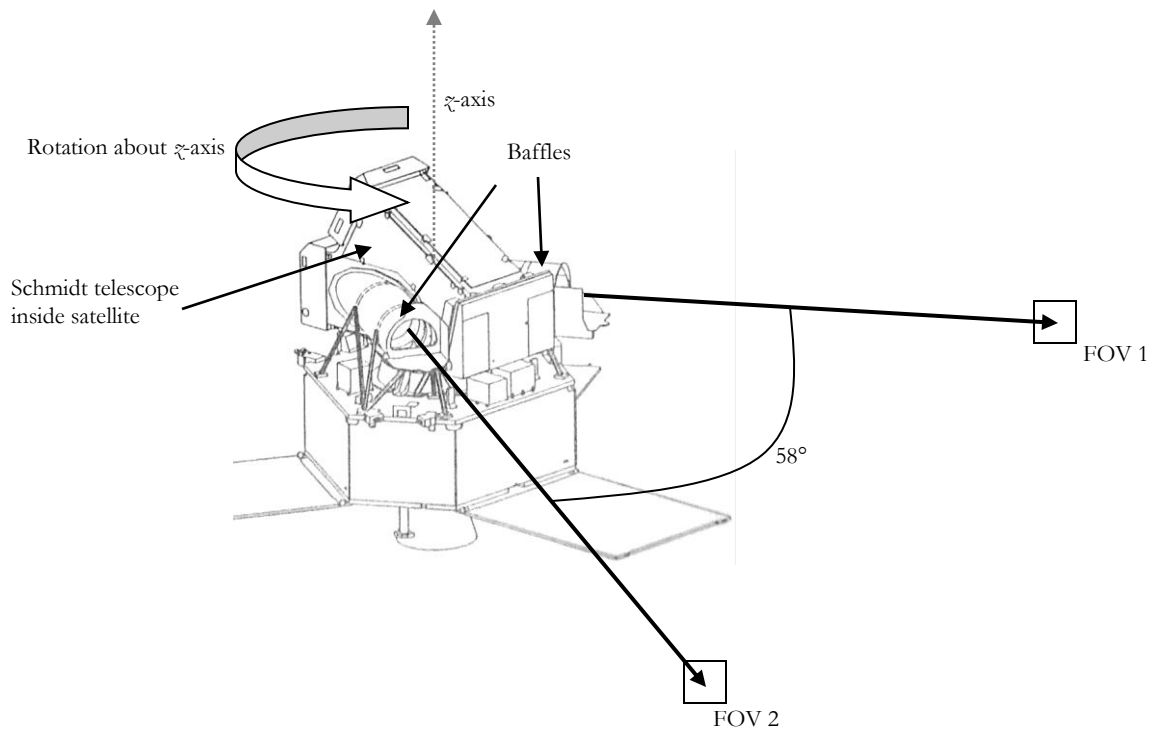


Figure 4. Hipparcos' fields of view and rotation [3]. Two fields of view separated by  $58^\circ$  have their light combined on the spherical primary mirror of the Schmidt telescope. Those images are then compared to calculate the stars' angular separation.

At the focal plane of the primary mirror sat a modulating grid [3, 8, 14] consisting of 2,688 slits manufactured via electron lithography. The slits were oriented perpendicular to the direction of scanning, parallel to the  $z$ -axis, and were  $3.13 \mu\text{m}$  wide with a separation of  $8.20 \mu\text{m}$  measured from slit center to slit center. Their width and separation corresponded to  $0.461 \text{ arcsec}$  and  $1.208 \text{ arcsec}$ , respectively, at a focal length of  $1.4 \text{ m}$ —the nominal focal length. As the star light shined through the grid it was intermittently blocked and unblocked by the slits. Viewed from behind the grid it therefore pulsed at  $140 \text{ Hz}$  and was sampled by an image dissector tube at  $1,200 \text{ Hz}$  using photon counting as a means to determine magnitude and angular separation. The image dissector tube was simply a photomultiplier tube. A star's photoelectron counts were used to derive its phase and the difference in phase between two stars was used to derive their angular separation as illustrated in Figure 5. Phase can be thought of in the following way. As a star's light was intermittently blocked and unblocked by the slits a periodic function was produced of intensity (photon counts) versus time. If such histograms of two stars did not have peaks and troughs at the same time they were not in phase, and this is called the phase difference. Furthermore, each star was measured for an integer

number of slits. This eliminated the possibility that a star would be some unknown distance between slits when photon counts started or ended for a particular star.

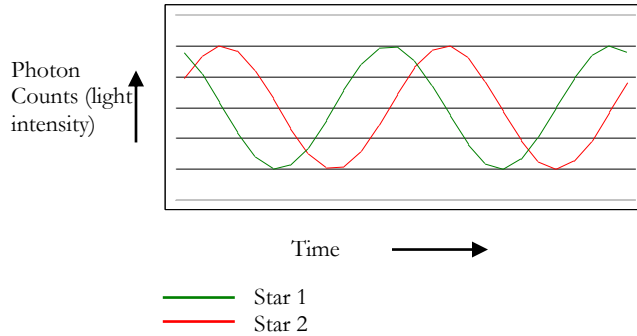


Figure 5. Plot showing phase difference of stars. This shows nominal star/phase separation from near-simultaneous transit of two stars. The stars are blocked by the slits at different times.

The image dissector tube could only track one star at a time, so it was not theoretically possible to measure multiple stars' phases and magnitudes simultaneously. To circumvent this a computer-controlled switching mirror rapidly switched between program stars in the field of view, thereby sending light from only one star at a time to the image dissector tube. To a reasonable level of certainty it was known which program stars would cross the field of view at a certain time, and this *a priori* information was transmitted from the ground to the spacecraft at regular intervals. Thus an observing scheme was planned before each program star transit to determine the order of switching for the mirror and the subsequent measurement by the image dissector tube.

### 3.4 Tycho Experiment

One year after ESA approved Hipparcos, E. Høg realized and submitted the proposal [13] to ESA that the star-mapper could also be used for ascertaining the photometric and astrometric properties of stars—stars that later found themselves in the Tycho Input Catalogue. This Tycho Experiment sought to produce a catalogue containing corresponding magnitudes and astrometric positions.

In order for the switch mirror to accurately send starlight from the program stars to the image dissector tube, the spacecraft's attitude [15] had to be known to 1 arcsec precision at

the time of the measurement—the 1 arcsec precision could not have been later calculated during analysis since the attitude data was needed in real-time to control the switch mirror. This attitude was determined by the onboard computer. The instrument partially responsible for attitude determination—in addition to the gyroscopes and program star file—was the star-mapper [8, 13, 15]. As shown in Figure 6, the star-mapper required the use of a second grid set, next to the main grid at the spherical mirror prime focus, and to be useful to the Tycho Experiment, the addition of a dichroic beam splitter and a pair of photomultiplier tubes. Each component was supplied in double redundancy.

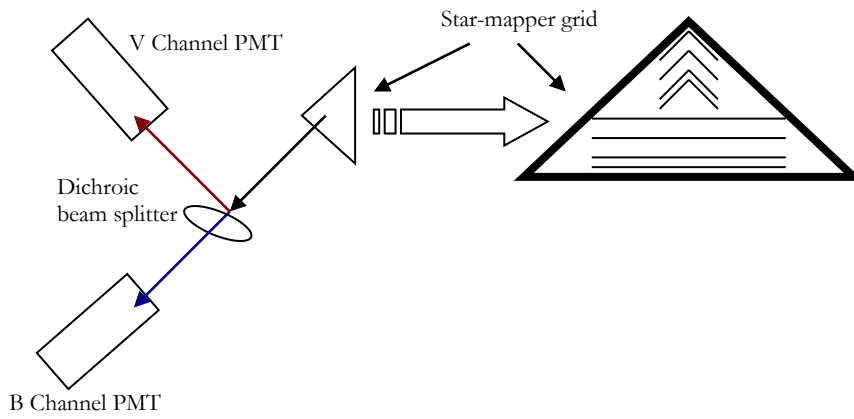


Figure 6. Tycho/star-mapper schematic. Light from the spherical mirror enters the star-mapper grid (enlarged on right to show slits) and passes through the dichroic beam splitter. Predominantly blue light (B channel) is transmitted to a photomultiplier tube (PMT) and broad spectrum visible light (V channel) is reflected to a PMT [8,15].

The second grid featured two kinds of slits: slits perpendicular to the scanning direction and chevron-shaped slits at a  $\pm 45$ -degree angle to the same. There were four slits of each type. The chevron slits allowed for determination of the two-dimensional stellar motion, rather than the one dimensional motion observable on the main grid. Prisms directed the light to both the main grid and the star-mapper grid.

After passing through the star-mapper grid the light came to a dichroic beam splitter. The dichroic beam splitter transmitted light in wavelength ranges of  $430 \pm 90$  nm (the blue or “B” channel) and it reflected light in wavelength ranges of  $530 \pm 100$  nm (the visual or “V” channel). The transmitted and reflected light went to the photomultiplier tubes which sampled at 600 Hz.

### 3.5 Support Systems

The support systems [3] onboard the Hipparcos satellite provided the logistical support for all aspects of spacecraft and science operations. As partially illustrated in Figure 7 they consist of the following systems.

#### 3.5.1 Attitude and Maneuvering

Hipparcos used two thruster systems: a “hot gas” and “cold gas” architecture. Both were monopropellant; the hot gas system used hydrazine ( $N_2H_4$ ). The hot gas system was only used in the first phase of the mission to initialize the satellite—that is, to make the appropriate transitions from the launch phase to the data collection phase. When no longer needed, the remaining hydrazine was vented into space to empty the tanks and so increase the pointing accuracy of the telescope by eliminating the potential for liquid slosh.

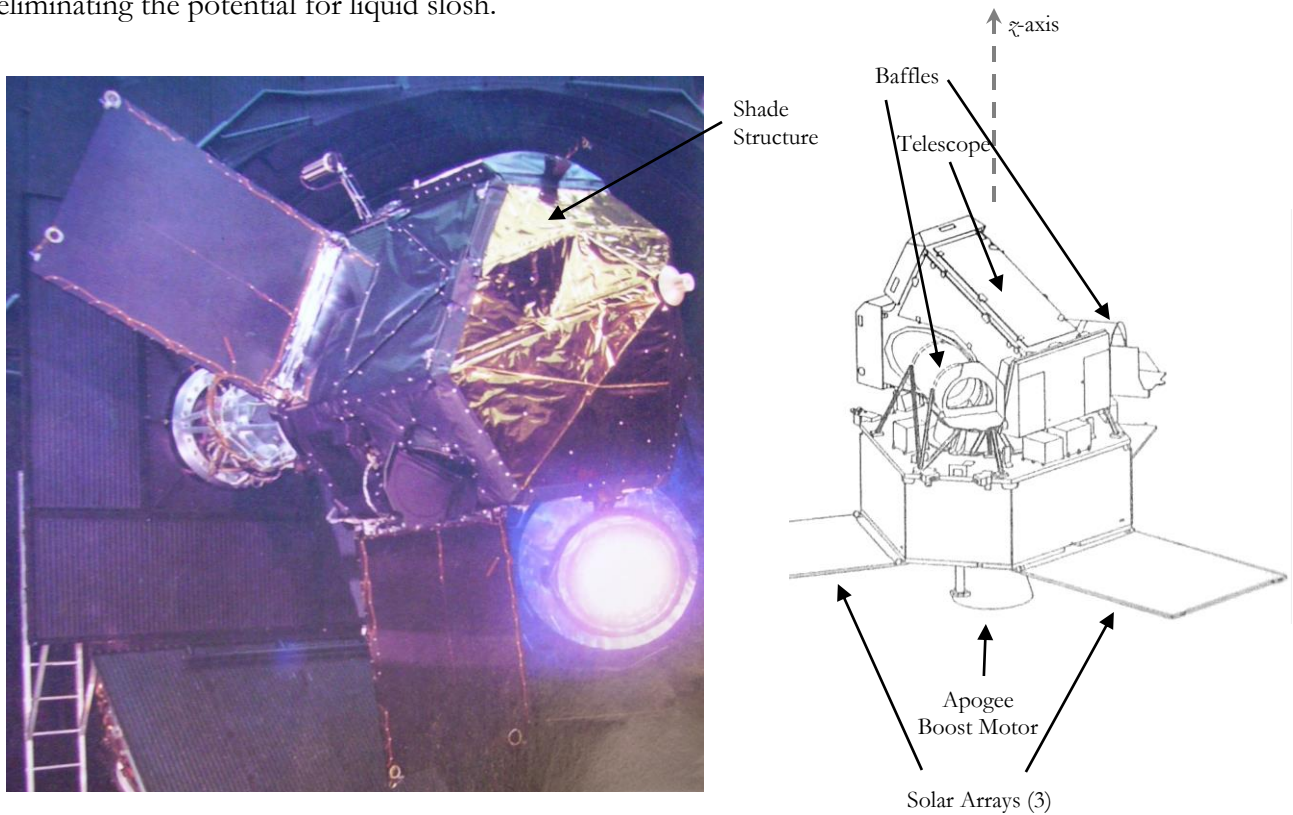


Figure 7. A photograph and sketch of the Hipparcos Satellite [3]. The sketch shows the spacecraft without the gold and black shade structure as seen in the photograph.



Precise control of the satellite's attitude was crucial in the operational mission phase for stable telescope pointing and calibration. Attitude control of the spacecraft was achieved via the firing of 20 mN cold nitrogen gas thrusters with a specific impulse between 60 and 70 s. Two non-interconnected gaseous nitrogen tanks supplied gas to six thrusters with the possibility of supplying six redundant thrusters. Given the need for a very steady observing platform, these proved the least jittery and were chosen over reaction control gyroscopes or magnetic torquers. (The latter device would have used magnetic coils and Earth's magnetic field to create torque, but this method is subject to unpredictable fluctuations in Earth's magnetic field.) Gas thrusters only disturbed observations for two seconds out of every 400 seconds, on average, which was short compared to the observing time. At the beginning of the mission, the spacecraft carried 9.4 kg of useable nitrogen stored at a pressure of 285 bar in two equally sized tanks.

A MAGE 2 apogee boost motor was intended to circularize the orbit of Hipparcos into a geostationary orbit from its initial transfer orbit. The boost motor contained 461.75 kg of solid aluminum composite propellant belonging to the flexadyne propellant family and was rated at a maximum thrust of over 40 kN with a burn phase of approximately 40 s and a specific impulse of 293 s.

### 3.5.2 Telecommunication

The spacecraft received telecommands at 2 kbits s<sup>-1</sup>. Telemetry from Hipparcos was designed to be downlinked at 1.44 kbits s<sup>-1</sup> in the transfer orbit and 23.04 kbits s<sup>-1</sup> in the geostationary orbit. The reviewed literature does not seem to indicate if the spacecraft communicated at a higher data rate after the failure of the apogee boost motor. The design constraints considered for the communications system included the requirement for ground-based computers to uplink data to the satellite, in addition to the obvious need to transmit scientific and engineering data to the ground. Specifically, the communication requirements necessitated the ability to uplink up-to-date program star files to plan observations and send 150 Hz synchronizing pulses to the payload computers. The original plans called for one ground station since the satellite would be in a geostationary orbit and therefore not to move in Earth's sky. Two additional ground stations [7] were added after the spacecraft did not enter the planned orbit.

### 3.5.3 Thermal Control

To minimize temperature variations throughout the spacecraft—particularly the electronics—insulators, radiators, and heaters worked to keep the temperature stable. Passive temperature control was utilized as much as was feasible by employing shade structures, multi-layer insulation, and black-painted surfaces. Except for some radiators to dissipate internal heat, the spacecraft components were thermally decoupled from hot or cold external environments with insulation and shading. The radiators were honeycomb panels with one side painted black and the other side having optical solar reflectors.

For cold mission phases—such as when the spacecraft was in Earth’s shadow—heat dissipated from the batteries worked to keep components above their minimum operating temperature. The minimum temperature ranged from  $-10^{\circ}\text{C}$  to  $+9^{\circ}\text{C}$ , depending on the component in question. When heat from the batteries was insufficient, battery heaters would activate to keep them at a temperature of  $-10^{\circ}\text{C}$ .

### 3.5.4 Power Generation and Management

Three photovoltaic solar array wings, each of dimensions 1.69 m long, 1.19 m wide, and 2.3 cm high, provided electrical power to the spacecraft when it was in sunlight as well as to charge two nickel cadmium batteries. The satellite systems were designed to run on 50V DC, providing a minimum of 85 W from either the solar arrays or the batteries. Each solar array had two general sections: a main section (subdivided into two subsections) and a charge section (divided similarly). The main sections provided the nominal 50V DC necessary to run satellite systems, and each solar array section could provide up to 125 W. The charge sections were dedicated to trickle-charging the batteries, though they could supplement the main sections if necessary. Each main subsection had seven strings made up of 142 serially connected photovoltaic cells with blocking and shunt diodes for protection. Each charge subsection had 126 serial connected cells, again with blocking and shunt diodes. Structurally, the solar arrays used a honeycomb structure of aluminum and carbon fiber reinforced plastic.

The batteries were kept at full charge during sunlit mission phases. Discharge regulators controlled the power from the batteries and were not supposed to supply more than 304 W. Battery current output was limited to  $2.5 \pm 0.25$  A and the total battery capacity was 720 Watt-hours when fully

charged in sunlight and, when discharged to a depth of 65%, was 468 Watt-hours in Earth's shadow. The transition from solar array to battery power was done automatically via a shunt regulator circuit.

A concern of solar-powered spacecraft is the build-up of charge and the eventual discharge of non-conducting surfaces. To mitigate against this threat, nearly the entire exterior of the spacecraft was electrically conductive, including the painted regions. However, the front sides of the solar arrays were non-conducting, but were protected with aluminized Kapton foil and grounded to the solar array structure. Shunt diodes—diodes that provide an alternate path for current in the event of a circuit failure—were incorporated to protect the arrays in the event that the inner parts of the arrays were shadowed due to an attitude control failure.

### 3.5.5 Gyroscopes

Five gyroscopes [3, 16] were used in calculating the orientation of the spacecraft (though not used in positioning the spacecraft). Two were along the  $z$ -axis and the other three were in the  $xy$  plane. Gyroscope and star tracker information was relayed to the ground for real-time determination of the satellite attitude.

## 3.6 The Hipparcos Launch and Mission Performance

Hipparcos was launched [16, 17] from ESA's French Guiana launch site on August 8, 1989 on an Ariane 4 rocket. It was placed into an eccentric geostationary transfer orbit, but, as has been mentioned, the apogee boost motor failed and the satellite stayed in its transfer orbit. This required the addition of two additional telemetry control stations as well as major software modifications. Despite these setbacks, and even before all the mission modifications had been implemented, normal operations began on November 27 of the same year. By May of 1990 the Goldstone Deep Space Communications Complex in California, part of NASA's Deep Space Network, became available for use in Hipparcos' mission.

The mission ended in August of 1993 after 37 months of effective observation time. The mission could have theoretically lasted into mid-1994 or 1995 based on the quantity of gas for the attitude control system, but the onboard computer failed outright in 1993 and the guidance system faced major problems. Just prior to these failures the onboard  $x$ -axis gyroscopes began failing, putting the spacecraft in a Sun-pointing attitude unfit for data collection.

DATA REDUCTIONS – NDAC, FAST, AND TYCHO

In order to ensure proper reduction of Hipparcos’ data, two independent consortia were organized: the Northern Data Analysis Consortium (NDAC) [14] led by L. Lindegren of Sweden and the Fundamental Astrometry by Space Techniques (FAST) [18] consortium led by J. Kovalevsky of France. A third Tycho catalogue [13, 19] was produced as a result of the Tycho experiment to determine photometric properties of stars.

#### 4.1 NDAC

Satellite data were received from the European Space Operations Centre (ESOC) in Darmstadt, Germany and sent to the Royal Greenwich Observatory (RGO) in England for initial processing. This processing at RGO involved first determining the celestial coordinates of the instrument axes—the spacecraft’s attitude—as a function of time to an accuracy of  $\sim 0.1$  arcsec. The attitude determination allowed knowledge of where each telescope baffle pointed at the time of a stellar transit across the star-mapper slits. The integral of three of the five gyroscope readings determined the spacecraft’s attitude, using a star mapper transit from each FOV to fix the constants of integration. Second, the instantaneous one-dimensional star positions on the modulating grid were deduced—the grid coordinates. RGO also performed photometric calibration of the detectors so that all the observed stars’ magnitudes could be accurately estimated.

From RGO the data were sent to Copenhagen University Observatory (CUO) for great-circle reductions. This determined each stars’ one-dimensional position (called abscissae) along specific or reference great-circles in terms of an angular coordinate; it “translated” the grid coordinate to a coordinate on a great circle. The interval of time during the mission when observations along one whole great circle were made and reduced as a set was called a “great-circle set.” Hipparcos rotated once about its  $\hat{x}$ -axis every 128 minutes, but this axis precessed at a rate of  $11 \text{ arcmin hr}^{-1}$ . The mean direction of Hipparcos’  $\hat{x}$ -axis during the time span of each great-circle set defined the pole, denoted  $\mathbf{r}$ , of the great-circle under consideration. The mean direction was required since Hipparcos’ rotation axis precessed. Great-circle sets of about 8 hours became the norm and were dictated by Hipparcos’ elliptical orbit which carried it through the van Allen radiation belts. The radiation belts added noise

by triggering the PMTs and interfering with other electronics and thereby decreased the signal-to-noise ratio. If great-circle sets were greater than 12 hours there would be too much discrepancy between the true rotation axis and  $\mathbf{r}$  because of the precession; if they were less than 4 hours it would be too difficult to determine the field-to-grid transformations based on a 24 term polynomial used to determine the same. Great-circle sets were therefore chosen to be about 8 hours long, which corresponded to the time when the spacecraft was away from its perigee and the radiation belts.

These data finally went to Lund Observatory in Sweden. CUO's determinations of abscissae were combined into a consistent all-sky sphere solution which included information on stars' parallaxes, proper motions, and positions.

In order to approach the theoretical limit of accuracy, these three broad steps (attitude determination, great-circle reductions, and the sphere solution) were iterated. The NDAC catalogue was then rotated to a final conventional coordinate system—called the FK5 system—by a uniform rigid rotation of the reference frame. This final NDAC catalogue was much improved over the original Input Catalogue, which had a positional accuracy of only 0.3 arcsec.

## 4.2 FAST

The FAST consortium, established in 1976, also used an iterative reduction process. Starting with the Input Catalogue of program stars, the positions of stars were refined from initial Hipparcos data. This reduced the error of the Input Catalogue by a factor of 15. This new solution was then reduced anew, using the corrections made to the Input Catalogue from the previous iteration. The FAST reduction flow could be divided into four main parts: first look and calibration, first treatment, synthesis treatment, and iteration. FAST did the bulk of the data reduction automatically using what was called the Data Management and Command Software (DMCS).

ESA as well as the FAST Consortium wanted to have some preliminary results shortly after each set of data were obtained. As such, DMCS could not be used and so a new phase of processing was created, called first look and calibration. In this phase large scale transformations from the grid to the field of view were made, as were main grid photometric calibrations and star-mapper calibrations.

In the “first treatment” phase, the data were collected and organized into batches that could be analyzed *en masse*. Next, the satellite’s attitude was determined using the star-mapper data exclusively. Analyses done at Centro di Studi sui Sistemi in Torino indicated the on-board gyroscopes were relatively useless compared to attitude determinations based on the timings of star crossings in the star-mapper. A rough idea of Hipparcos’ attitude was made using the Input Catalogue star positions, but this was refined iteratively. Next came the task of finding the grid coordinates of each transiting star using the star intensity modulation and grid phase relation

$$I = I_0 + B + I_0 M_1 \cos(\omega t + \Phi_1) + I_0 M_2 \cos 2(\omega t + \Phi_2) \quad \text{Eq. 2}$$

where  $I_0$  is the star’s intensity,  $B$  is the background,  $M_1$  and  $M_2$  are modulation coefficients and depend on a star’s color since different wavelengths affect diffraction,  $\Phi_1$  and  $\Phi_2$  are the phases at the mean time during an observation, and  $\omega$  is a star’s linear velocity on the grid which depends on the derivative of the spacecraft’s position (attitude). The five parameters of Equation 2 needed to be found for each star, and for purposes of linearization the following were chosen as unknowns:

$$I_0 + B; \quad I_0 M_1 \cos \Phi_1; \quad I_0 M_1 \sin \Phi_1; \quad I_0 M_2 \cos 2\Phi_2; \quad I_0 M_2 \sin 2\Phi_2.$$

The final step in first treatment is the great-circle reductions using the attitude and grid coordinates (to find the abscissae), and the Input Catalogue’s ordinate. The ordinate, since it came from the Input Catalogue, had a large error but was corrected using spacecraft attitude data as much as possible and was later refined iteratively.

The next step, the “synthesis treatment,” finalized one iteration of the reduction cycle by finding the sphere solution and finally the complete astrometric parameters. The sphere solution was a set of reference great-circles with known poles and origins. Once the sphere solution was complete, software was used to recognize and correct for grid step error (if a star had a miscalculated grid coordinate) and the peculiar motions caused by double or multiple stars. Astronomisches Rechen-Institut in Heidelberg (ARI) performed a re-treatment of double and multiple stars to correct for their motion about one another and thereby find one astrometric parameter for a fixed point in the system. FAST scientists then determined which results showed a significant improvement over the previous astrometric parameters. The output catalogue was produced thusly.

The last step was called “iterations.” This simply means that the previous step, “synthesis treatment,” was repeated, using as its input the output from the previous iteration to obtain higher-

quality data. At the end of each iteration the FAST data were compared with NDAC and with ground-based determination of radio stars from very long baseline interferometry (VLBI); any necessary software improvements were implemented. Generally, FAST and NDAC differences were minor. The final output catalogue was then combined with the results from NDAC to produce the final Hipparcos Catalogue.

### 4.3 The Hipparcos Catalog

The results from NDAC and FAST were compiled [20] into the complete Hipparcos Catalogue which became available to the general astronomical community in June of 1997 [12]. As taken from Mignard [16], the pertinent properties of the Hipparcos Catalogue are shown in Table 1.

Measurement Period	1989.85-1993.21
Mean-Sky Density	$\sim 3$ stars/deg <sup>2</sup>
Number of astrometric solutions	117,955
Systematic Errors	$< 0.1$ mas

Table 1. Pertinent properties from the Hipparcos Satellite.

### 4.4 Tycho

The Tycho Catalogue [13, 19] of astrometric and photometric parameters of 1,058,332 stars was published in 1997. Like the Input Catalogue for the Hipparcos experiment, the Tycho experiment also used an Input Catalogue. This catalogue was a merger of the Hubble Space Telescope (HST) Guide Star Catalogue and the Hipparcos Input Catalogue and consisted of 3 million of the brightest stars in the sky. Recall from Section 3.4 that light was split by a dichroic beam splitter to roughly blue (B) and visible (V) light channels. The minimum stellar magnitude for B was 12.8 mag and for V was 12.1 mag. The error in magnitudes for the photometric determination ranged between 0.003 mag and 0.012 mag.

## DATA APPLICATIONS FROM THE HIPPARCOS SATELLITE

The uniquely accurate astrometric measurements from Hipparcos have allowed the Hipparcos data to be used in a wide range of applications. Several examples are presented below, ranging from testing stellar interior theory [5] to climatology [6]. One example [21] serves as checks for Hipparcos data

### 5.1 Interferometric Angular Diameters of Mira Variables with the Hubble Space Telescope

Lattanzi *et al.* [21] used the Fine Guidance Sensor (FGS) aboard HST to measure the sizes of the stellar discs of the stars R Leonis and W Hydrae. These two stars are Mira variables with periods of 312 and 373 days, respectively. The group discovered asymmetries in the two stars such that their minor axes were about 11% and 20% of their major axes, respectively. They point out that these asymmetries, which are also variable, may call into question the accuracy of the positions, proper motions, parallaxes, and even sizes of Mira variable stars observed by Hipparcos.

### 5.2 Galactic Kinematics of Cepheids from Hipparcos Proper Motions

Feast and Whitelock [1] describe how stellar proper motions obtained from parallax measurements taken from Hipparcos are in agreement with proper motions derived using radial velocity for the same stars. Of significance is the derived distance of the Sun from the galactic center implied by the Oort Constant  $\mathcal{A}$ , which is

$$A = -\frac{1}{2}R_0 \left( \frac{d\Omega}{dR} \right)_0 \quad \text{Eq. 3}$$

where the subscript “0” indicates a value at the Sun’s galactic position,  $R$  is the distance to the galactic center, and  $\Omega$  is the angular velocity of the Sun about the galactic center. The units of  $\mathcal{A}$  are  $\text{km s}^{-1} \text{kpc}^{-1}$ . The calculated distance is

$$R_0 = 8.5 \pm 0.5 \text{ kpc.}$$

The authors thereby further establish the accuracy of the Hipparcos results, especially as pertains to proper motions.



### 5.3 Ages of Globular Clusters from Hipparcos Parallaxes of Local Subdwarfs

Gratton *et al.* [22] used Hipparcos parallax data of subdwarf stars, coupled with high-resolution spectroscopy, to determine absolute ages for Galactic globular clusters (GGCs) and the implications for cosmology. The distance-spectroscopy study led the team to determine the absolute location of the main sequence as a function of metallicity. Generally, younger generation stars are more metal-rich (a metal being defined as any element heavier than helium), having been enriched by previous generations of stars. If a small, old, long-lived star on the main sequence has certain metals in it, it implies those metals are primordial—created shortly after the Big Bang. These results allowed the team to determine the distances and ages for nine globular clusters. The ages were determined to within 1.5 billion years. Their ages were then used to compute an age for the universe of 12.3 billion years. Based on their computed ages for globular clusters, they concluded that standard inflationary Big Bang models of the universe are not undermined.

### 5.4 The Mass and Radius of 40 Eridani B From Hipparcos: An Accurate Test of Stellar Interior Theory

Shipman *et al.* [5] used the Hipparcos parallax-derived distance to the white dwarf 40 Eridani B to determine properties of the star as a test of stellar degeneracy theory. Not many data points have become available to test stellar degeneracy theory, but the better-than-1% distance accuracy data from Hipparcos add several. 40 Eri B has a companion star, and for visual binaries the mass of the two bodies is strongly correlated to the parallax angle  $\pi$  between them as they orbit their center of mass:

$$M \propto \pi^{-3}.$$

The mass was determined to be  $M = 0.501 \pm 0.011$  solar masses and the radius to be  $R = 0.0136 \pm 0.00024$  solar radii. This is consistent with single-star evolution and does not require any additional evolutionary models to explain the data.

Hipparcos measured a parallax angle of  $198 \pm 0.84$  mas, which was smaller than previously used ground-based parallax of  $207 \pm 2$  mas. Using Equation 1, the Hipparcos parallax puts 40 Eridani B at a distance from Earth of  $5.05 \pm 0.02$  pc, or about 16.4 light years.

## 5.5 The Hipparcos Distances of Open Clusters and their Implication on the Local Variations of the $\Delta X/\Delta Z$ Ratio

Due to parallax results from Hipparcos, Efremov *et al.* [23] report that distance scales within the Milky Way are shorter than earlier thought. This has implications for the luminosities of stars—specifically that they should be dimmer than previously thought—and that, in particular, the period-luminosity relation for Cepheid variables is somewhat different than previously thought. As such, Cepheid variable standard candles are more precisely calibrated.

The  $\Delta X/\Delta Z$  ratio is the ratio between helium and metal abundance in the interstellar medium (ISM). The new parallax-measured distances, coupled with luminosity and stellar mass information, aided the determination of helium and metal abundances around stars and in stellar systems. This study found that there is seemingly no universal correlation of helium and metal abundances.

## 5.6 Seismic Analysis of the Planet-Hosting Star $\mu$ Arae

Bazot *et al.* [24] attempted to determine the nature of  $\mu$  Arae’s metallicity. This star hosts exoplanets and like other exoplanet-hosting stars its spectrum shows an abundance of metals. An attempt was made to use asteroseismic analysis to determine if the metals were primordial in nature—and therefore distributed throughout the star—or if they were the result of the star’s accretion history and therefore be only in the outer layers. Asteroseismic analysis uses spectroscopy to study the Doppler shift due to oscillations of a star’s surface. Determination of the precise location of the star on the HR diagram was aided by accurate knowledge of its parallax taken from Hipparcos since more accurate distance information yields more accurate luminosities. The HR diagram location was further constrained by the seismic analysis which discriminated between the two metallicity scenarios. The nature of  $\mu$  Arae’s metallicity was inconclusive, but in the process a 14-Earth mass exoplanet was discovered orbiting the star.

## 5.7 Ice Age Epochs and the Sun’s Path Through the Galaxy

Gies and Helsel [6] used Hipparcos data to derive speed and position data for the Sun to calculate the Sun’s path through the Milky Way Galaxy over the past 500 million years. They assumed a spiral pattern speed of 14-17 km s<sup>-1</sup> kpc<sup>-1</sup> and used what they considered to be a realistic model for the Galaxy gravitational potential in their calculation. (It should be noted that the authors draw attention

to a more recent calculation of Galactic dynamics which indicates a spiral pattern speed closer to  $20 \pm 5 \text{ km s}^{-1} \text{ kpc}^{-1}$ .) They point out a strong correlation in the last 500 million years between the past four long-term ice ages in Earth's history with the past four passages of the Sun through the Galaxy's spiral arms. Nebulae and supernova events are more common in the spiral arms due to the higher density of material, and as Earth passes through this denser medium an increase in the cosmic-ray flux (CRF) through Earth's atmosphere results. Cosmic rays can serve as nucleation sites for cloud condensation, increasing low altitude cloud cover and contributing to global cooling. The authors cite research by Marsh and Svensmark [25] showing a strong correlation between CRF and low altitude cloud coverage over 15 years.

FUTURE PROSPECTS AND CONCLUSION

**6.1 Future Prospects**

To build on the success of Hipparcos, ESA is currently developing a follow-on mission, called Gaia [26, 27, 28]. Gaia originally was an acronym which stood for Global Astrometric Interferometer for Astrophysics, but as mission planning continued it became clear Gaia would do more than interferometry. Gaia is scheduled to launch in 2011 on a Russian Soyuz rocket from ESA's French Guiana launch site and orbit the Sun at the second Sun-Earth Lagrange point 1.5 million kilometers from Earth. The basic operating principle will be the same as Hipparcos but will take advantage of improved technology, including improved detectors, computers, and the advent of silicon carbide-enhanced optics. Two telescopes, each with a diameter of 1.45 m, will focus the light from two fields of view onto a focal plane with various detectors.

Gaia is expected to produce a catalog of approximately one billion stars and solar system objects down to 15 mag and 24 microarcsec positional accuracy over a five year prime mission, producing a thousand times more data than Hipparcos. Gaia will be so sensitive as to be able to ascertain the bending of starlight from the Sun as a test of General Relativity, directly determine the distance—via parallax—to the Magellanic Clouds, determine masses of exoplanets down to 10 Earth masses, and, possibly, provide indirect evidence for gravitational waves.

**6.2 Conclusion**

ESA's Hipparcos astrometry satellite, designed to find astrometric positions of 120,000 program stars, calculate their parallax, and find the photometric properties of a million stars, succeeded in its mission. Not only did it succeed, but it did so to a higher degree of precision [27] than anticipated during its program acceptance and planning phase in 1980, despite being left in a orbit drastically different than originally planned. The final products—the Hipparcos and Tycho Catalogues—are the result of processing 100 Gbits of satellite data.

The astrometric and photometric results have aided astronomers in many sub-disciplines of astronomy, including cosmochemistry and even climatology. Further refinements to data and several

new discoveries await the ultra-precision and large data volumes to be gathered by Gaia starting in 2011.

## References

- 
- [1] M. Feast and P. Whitelock, *Monthly Notices of the Royal Astronomical Society*, **291**, 683-693 (1997).
- [2] Bazot *et al.*, *Astron. Astrophys.*, **440**, 615-621 (2005).
- [3] The Hipparcos Mission. Prelaunch Status. Volume 1: The Hipparcos Satellite. ESA Publications Division (1989).
- [4] S. Vasilevski, *Annu. Rev. Astron. Astrophys.*, **4**, 57-76 (1966).
- [5] H.L. Shipman, *et al.*, *Astrophys. J.*, **488**, L43-L46 (1997).
- [6] D.R. Gies and J. W. Helsel, *Astrophys. J.*, **626**, 844-848 (2005).
- [7] J. Kovalevsky, M. Froeschlé, Proceedings of the 156<sup>th</sup> Symposium of the International Astronomical Union, Kluwer Academic Publishers, 1-10 (1993).
- [8] M.A.C. Perryman, *Nature*, **340**, 111-116 (1989).
- [9] *ESA, Hipparcos Scientific Involvement*, <[http://www.rssd.esa.int/SA-general/Projects/Hipparcos/CATALOGUE\\_VOL1/scientific\\_involvement.ps.gz](http://www.rssd.esa.int/SA-general/Projects/Hipparcos/CATALOGUE_VOL1/scientific_involvement.ps.gz)>, accessed 3/24/2008.
- [10] *Greenwich Observatory, Green Witch Newsletter*, <<http://green-witch.com/newsletter26.html>>, accessed 3/24/2008.
- [11] *ESA Science and Technology*, <<http://hipparcos.esa.int/science-e/www/area/index.cfm?fareaid=20>>, accessed 3/24/2008.
- [12] F. Mignard, *New Horizons from Multi-Wavelength Sky Surveys*, 399-405 (1997).
- [13] E. Høg, *et al.*, *Astron. Astrophys.*, **258**, 177-185 (1992).
- [14] L. Lindegren *et al.*, *Astron. Astrophys.*, **258**, 18-30 (1992).
- [15] The Hipparcos Mission. Prelaunch Status. Volume 3: The Data Reductions. ESA Publications Division (1989).
- [16] F. Mignard, Proceedings of the International Astronomical Union, NASA Astrophysics Data System (1997).
- [17] J. Kovalevsky and M. Froeschlé, *Developments in Astrometry and Their Impact on Astrophysics and Geodynamics*, 1-10 (1993).
- [18] J. Kovalevsky, *et al.*, *Astron. Astrophys.*, **258**, 7-17 (1992).
- [19] E. Høg, *et al.*, *Astron. Astrophys.*, **323**, L57-L60 (1997).
- [20] *The Hipparcos Space Astrometry Mission: Research Tools* <[http://www.rssd.esa.int/index.php?project=HIPPARCOS&page=Research\\_tools](http://www.rssd.esa.int/index.php?project=HIPPARCOS&page=Research_tools)>, accessed 6/2/2008.
- [21] M. Lattanzi, *et al.*, *Astrophys. J.*, **485**, 328-332 (1997).
- [22] R.G. Gratton *et al.*, *Astrophys. J.*, **491**, 749-771 (1997).
- [23] Efremov *et al.*, *Astron. Nachr.*, **318**, 335-337 (1997).
- [24] Bazot *et al.*, *Astron. Astrophys.*, **440**, 615-621 (2005).
- [25] N. Marsh and H. Svensmark, *Space Sci. Rev.*, **00**, 1-16 (2000).
- [26] *ESA Space Science, Gaia*, <<http://www.esa.int/science/gaia>>, accessed 5/17/08.
- [27] M.A.C. Perryman, *Experimental Astronomy*, **7**, 325-328 (1997).
- [28] *Gaia Acronyms*, <<http://gaia.esac.esa.int/gpdb/glossary.txt>>, accessed 6/2/2008.